New Guidance and Control Techniques for Lunar Ascent and Orbit Injection

Mauro Pontani[1, a)]

Author Affiliations
[1]*Department of Astronautical, Electrical, and Energy Engineering, Sapienza Università di Roma, via Salaria 851, 00138 Rome, Italy*

Author Emails
[a)] Corresponding author: mauro.pontani@uniroma1.it

Abstract. This work deals with two distinct guidance and control architectures for autonomous lunar ascent and orbit injection: (i) Variable-Time-Domain Neighboring Optimal Guidance and Constrained Proportional Derivative attitude control (VTD-NOG&CPD) and (ii) locally-flat near-optimal guidance and nonlinear reduced-attitude control. While (i) represents a well-consolidated implicit-type guidance, briefly outlined in this work, (ii) is a new explicit guidance scheme, accompanied by a novel quaternion-based reduced-attitude control algorithm, which enjoys quasi-global stability properties. Attitude control is aimed at pursuing the desired thrust alignment, identified by the guidance algorithm. Actuation, based on thrust vectoring, is modeled as well. Extensive Monte Carlo simulations prove the effectiveness of the guidance, control, and actuation architecture proposed in this study for precise lunar orbit insertion, in the presence of nonnominal flight conditions.

INTRODUCTION

Traditionally, two different approaches to guidance exist. Explicit algorithms [1] stem from the idea of re-defining the flight trajectory at the beginning of each guidance interval, at which an updated trajectory (leading to the target final condition) is computed. Implicit algorithms [2] consider the perturbations from a specified nominal trajectory, and define the feedback control corrections aimed at maintaining the vehicle in the proximity of the nominal path. Neighboring optimal guidance (NOG) [3] can be regarded as an implicit guidance technique that relies on the analytical second-order optimality conditions, with the intent of finding the corrective control actions in the neighborhood of the reference (optimal) path. Although NOG schemes outperform all the explicit guidance algorithms, the latter have the great advantage of not requiring any nominal trajectory. Moreover, usually explicit guidance techniques are more robust than implicit algorithms.

The work that follows is aimed at (i) outlining VTD-NOG & CPD [4], a particular implementation of neighboring optimal guidance, accompanied by a constrained proportional derivative attitude control scheme, (ii) introducing a new explicit near-optimal guidance, based on the local projection of the position and velocity variables, (iii) formulating and addressing the reduced-attitude-control problem, and (iv) modeling the actuation dynamics, based on thrust vectoring. The explicit guidance, control, and actuation approach proposed in this study does not require the offline preliminary computation of any reference trajectory or quantity. Monte Carlo simulations are run, for the purpose of ascertaining the effectiveness and accuracy of the architecture at hand, in the presence of significant displacements from the nominal initial conditions.

SPACECRAFT DYNAMICS

The ascent vehicle is assumed to be subject only to the gravitational attraction of the Moon, whose mass distribution is assumed spherical. Moreover, the (nominal) propulsive thrust is continuous and has constant

magnitude *T*. The mass ratio, denoted with $x_7 = m/m_0$ (where m_0 is the initial mass) obeys $\dot{x}_7 = -n_0/c$, where n_0 is the initial thrust acceleration. The spacecraft dynamics is governed by the trajectory and attitude equations.

The ascent vehicle trajectory can be described in an inertial reference frame, associated with the right-hand sequence of unit vectors $(\hat{c}_1, \hat{c}_2, \hat{c}_3)$. Its origin is located at the center of the Moon, and the target orbit lies on the $(\hat{c}_1, \hat{c}_2)$-plane. The position can be identified by the following three variables: radius *r*, right ascension ξ, and declination ϕ [5]. The spacecraft velocity can be projected into the rotating frame $(\hat{r}, \hat{t}, \hat{n})$, where $\hat{r}$ is aligned with the position vector $\boldsymbol{r}$ and $\hat{t}$ is parallel to the $(\hat{c}_1, \hat{c}_2)$-plane (and in the direction of the spacecraft motion). The related components are denoted with (v_r, v_t, v_n) and termed respectively radial, transverse, and normal velocity component. The upper stage is controlled through the thrust direction, defined by the in-plane angle α and the out-of-plane angle β. The governing equations for $(r, \xi, \phi, v_r, v_t, v_n)$ are omitted for the sake of conciseness (cf. [5]).

The spacecraft instantaneous orientation is associated with the body frame. Its origin is in the center of mass of the vehicle, while its axes are aligned with the right-hand sequence of unit vectors $(\hat{\imath}, \hat{\jmath}, \hat{k})$, with $\hat{\imath}$ pointing toward the longitudinal axis. In this research, the attitude (referred to $(\hat{c}_1, \hat{c}_2, \hat{c}_3)$) is described through Euler parameters (quaternions), denoted with $\{q_0, \boldsymbol{q}\}$, where q_0 is the scalar part, whereas $\boldsymbol{q}$ is the (3×1)-vector part. The attitude kinematics equations [6] involve the time derivatives of the Euler parameters and the (3×1)-vector $\boldsymbol{\omega}$, which includes the components (along $(\hat{\imath}, \hat{\jmath}, \hat{k})$) of the angular velocity of the spacecraft with respect to $(\hat{c}_1, \hat{c}_2, \hat{c}_3)$. Let $\mathbf{J}_C^{(B)}$ denote the spacecraft inertia matrix with respect to center of mass C, resolved in $(\hat{\imath}, \hat{\jmath}, \hat{k})$. The attitude dynamics equations are

$$\dot{\boldsymbol{\omega}} = \left[\mathbf{J}_C^{(B)}\right]^{-1}\left(-\tilde{\boldsymbol{\omega}}\mathbf{J}_C^{(B)}\boldsymbol{\omega} - \dot{\mathbf{J}}_C^{(B)}\boldsymbol{\omega} + \boldsymbol{T}_C\right) \tag{1}$$

where the (3×1)-vector $\boldsymbol{T}_C$ includes the (internal) torque components (along $(\hat{\imath}, \hat{\jmath}, \hat{k})$) due to thrust misalignment. In Eq. (1), $\dot{\mathbf{J}}_C^{(B)}$ is the time derivative of the inertia matrix, which is nonzero due to propellant consumption.

OUTLINE OF THE IMPLICIT VARIABLE-TIME-DOMAIN NEIGHBORING OPTIMAL GUIDANCE AND CONSTRAINED ATTITUDE CONTROL

Neighboring optimal guidance (NOG) schemes are based on minimizing the second differential of an objective function, typically propellant consumption or time of flight. This minimization principle leads to deriving all the corrective maneuvers.

Most recently, VTD-NOG [4] emerged as an effective algorithm, capable of circumventing the major difficulties of former contributions focused on NOG. In fact, a normalized time scale is adopted as the domain in which the nominal trajectory is defined. This has three remarkable consequences: (i) the gain matrices remain finite for the entire time of flight, (ii) the updating law for the time of flight derives directly from the necessary conditions for optimality, and (iii) the termination corresponds to the upper bound of the normalized time domain. VTD-NOG identifies the trajectory corrections by assuming a thrust direction always aligned with the longitudinal axis of the spacecraft. In Ref. 4, the constrained proportional derivative algorithm (CPD) is employed for attitude control through thrust vectoring and side jets, and pursues this alignment condition.

This new guidance and control concept was applied to lunar ascent and orbit injection, with the intent of testing its capabilities, in the presence of several nonnominal flight conditions, such as incorrect initial position, propulsive fluctuations, and imperfect modeling of the mass distribution and variation. Extensive Monte Carlo simulations pointed out that orbit injection occurs with excellent accuracy, thus demonstrating that VTD-NOG & CPD indeed represents an effective methodology for the application at hand. All the numerical results are reported in Ref. 4.

EXPLICIT LOCALLY-FLAT NEAR-OPTIMAL GUIDANCE

This research introduces a near-optimal guidance scheme based on local projection of the spacecraft position and velocity, under the assumption that the instantaneous trajectory is sufficiently close to the $(\hat{c}_1, \hat{c}_2)$-plane, which contains the target path. This is assumed to be an elliptic orbit about the Moon, with specified periselenium and aposelenum radii, denoted with r_A and r_P, respectively. Orbit injection is assumed to occur at periselenium.

The guidance algorithm is run repeatedly and starts at equally-spaced times $\{t_k\}_{k=0,\ldots,N-1}$; Δt_S denotes the sampling time interval. At t_k, the spacecraft position and velocity are projected onto the $(\hat{x}_k, \hat{y}_k, \hat{z}_k)$-frame, obtained from $(\hat{c}_1, \hat{c}_2, \hat{c}_3)$ through a single counterclockwise rotation by angle ξ_k, and yield the flat coordinates

$$x_k = r_k \cos\phi_k \quad y_k = 0 \quad z_k = r_k \sin\phi_k \quad v_{x,k} = v_{r,k}\cos\phi_k - v_{n,k}\sin\phi_k \quad v_{y,k} = v_{t,k} \quad v_{z,k} = v_{r,k}\sin\phi_k + v_{n,k}\cos\phi_k \tag{2}$$

These are governed by [5]

$$\dot{x} = v_x \quad \dot{y} = v_y \quad \dot{z} = v_z \quad \dot{v}_x = \tilde{a}_T \sin\theta_1 \cos\theta_2 - g \quad \dot{v}_y = \tilde{a}_T \cos\theta_1 \cos\theta_2 \quad \dot{v}_x = \tilde{a}_T \sin\theta_2 \tag{3}$$

where angles (θ_1, θ_2) identify the thrust direction in $(\hat{x}_k, \hat{y}_k, \hat{z}_k)$, g denotes the (local) gravitational acceleration, and $\tilde{a}_T$ is the thrust acceleration. Using (x, y, z, v_x, v_y, v_z), the desired conditions at orbit injection are

$$x_f = r_P \quad z_f = 0 \quad v_{x,f} = 0 \quad v_{y,f} = \sqrt{\frac{2\mu}{r_P + r_A}\frac{r_A}{r_P}} \quad v_{z,f} = 0 \tag{4}$$

The two optimal thrust angles (θ_1, θ_2) minimize the time of flight needed to fulfill the boundary conditions (4), while holding the state equations (3). The optimal control problem at hand is proven to be amenable to an analytical solution if $\tilde{a}_T$ and g are constant. All the state components (x, y, z, v_x, v_y, v_z) can be written as closed-form functions of time, depending on 5 unknown quantities. These are found as the numerical solution of 5 nonlinear equations, arising from enforcement of the boundary conditions (4). A suitable guess, related to intuitive variables, is available [5], and allows the real-time numerical solution of this nonlinear system. As a result, the commanded thurst direction is identified in each sampling interval $[t_k, t_{k+1}]$, and drives the attitude control system.

REDUCED-ATTITUDE CONTROL AND ACTUATION VIA THRUST VECTORING

Only the alignment of the longitudinal axis $\hat{\imath}$ with $\hat{\imath}^{(C)}$ is crucial for the purpose of pointing the thrust toward the correct direction. A reduced-attitude-tracking algorithm, aimed at pursuing the desired alignment for a single axis, is introduced in this research, as a suitable solution to the problem of interest. Let $\boldsymbol{\omega}_C$ and $\underset{B\leftarrow C}{\mathbf{R}}$ denote the commanded angular rate and the relative rotation matrix that relates the commanded attitude and the actual orientation; $\boldsymbol{\omega}_E := \boldsymbol{\omega} - \underset{B\leftarrow C}{\mathbf{R}}\,\boldsymbol{\omega}_C$; $\{q_0^{(E)}, q_1^{(E)}, q_2^{(E)}, q_3^{(E)}\}$ denotes the error quaternion. The feedback control law

$$\boldsymbol{T}_C = \tilde{\boldsymbol{\omega}}\mathbf{J}_C^{(B)}\boldsymbol{\omega} + \dot{\mathbf{J}}_C^{(B)}\boldsymbol{\omega} + \mathbf{J}_C^{(B)}\left[\underset{B\leftarrow C}{\mathbf{R}}\,\dot{\boldsymbol{\omega}}_C - \tilde{\boldsymbol{\omega}}_E \underset{B\leftarrow C}{\mathbf{R}}\,\boldsymbol{\omega}_C\right] - \mathbf{J}_C^{(B)}\mathbf{A}^{-1}\left[\mathbf{B}\boldsymbol{\omega}_E + \boldsymbol{f}\left(q_0^{(E)}, \boldsymbol{q}^{(E)}\right)\right], \tag{5}$$

with $\boldsymbol{f}\left(q_0^{(E)}, \boldsymbol{q}^{(E)}\right) := \left[0 \quad q_0^{(E)}q_2^{(E)} + q_1^{(E)}q_3^{(E)} \quad q_0^{(E)}q_3^{(E)} - q_1^{(E)}q_2^{(E)}\right]^T$, enjoys quasi global stability, i.e. it guarantees asymptotic convergence of the longitudinal axis of the ascent vehicle toward the commanded thrust direction. The two matrices **A** and **B** are constant and positive definite; **A** is also symmetric.

The preceding feedback control law yields the three torque components along the three body axes. However, the longitudinal component is ineffective for the purpose of thrust alignment, thus it is set to 0. The remaining two components are actuated using thrust vectoring. In particular the two components $T_{C,2}^{(C)}$ and $T_{C,3}^{(C)}$ yield the commanded deflection angles $\Delta_y^{(C)}$ and $\Delta_y^{(C)}$, using $T_{C,2}^{(C)} = Tl\cos\Delta_z^{(C)}\sin\Delta_y^{(C)}$ and $T_{C,3}^{(C)} = -Tl\sin\Delta_z^{(C)}$, where T is the thrust magnitude, whereas l is the distance from the center of mass to the nozzle. These commanded values for $\Delta_y^{(C)}$ and $\Delta_y^{(C)}$ are saturated to ± 5 deg. The real deflection mechanism, which yields the actual deflection angles, is modeled using a first-order system, with time coefficient set to 0.1 sec (cf. also [4]).

NUMERICAL SIMULATIONS

The ascent vehicle has initial mass of 4700 kg and principal inertia moments equal to $4800\ \mathrm{kg\,m^2}$, $9200\ \mathrm{kg\,m^2}$, and $8100\ \mathrm{kg\,m^2}$ [4]. The propulsion parameters are $n_0 = 0.5\ \mathrm{g}_0$ $\left(\mathrm{g}_0 = 9.8\ \mathrm{m/sec^2}\right)$ and $c = 3\ \mathrm{km/sec}$. Homogeneous mass depletion is assumed (and the center of mass does not move as a result). Aposelenium and periselenium have altitudes equal to 100 km and 15 km, respectively.

A Monte Carlo (MC) campaign is run, by assuming nonnominal flight conditions, namely (i) initial declination, with zero mean and standard deviation of 0.13 deg (corresponding to 4 km on the lunar surface), and (ii) propulsive fluctuations, modeled as in Ref. 4. Figure 1 illustrates the altitude and two components of the spacecraft velocity, obtained in the Monte Carlo campaign, composed of 100 simulations, using two distinct sampling intervals, i.e. 5 sec up to 250 sec after launch, and 0.5 sec for the remaining time. Inspection of the numerical results and the related statistics (omitted for the sake of conciseness) reveals that the guidance, control, and actuation architecture at hand is very effective for precise lunar orbit injection.

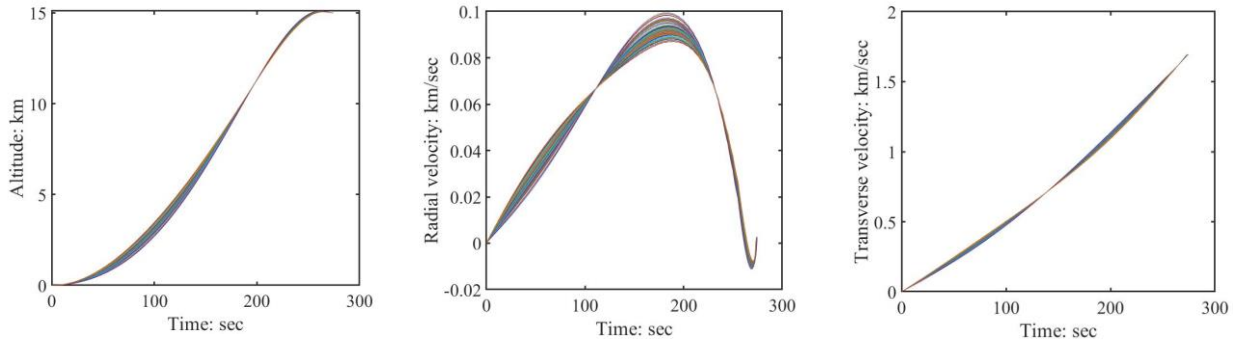

(a) (b) (c)

FIGURE 1. *Time histories of the altitude (a) and two components of the velocity (b,c), obtained in the MC campaign*

CONCLUSION

This research proposes a new guidance, control, and actuation architecture for autonomous lunar ascent and orbit injection. The locally-flat near-optimal guidance projects the spacecraft position and velocity into a convenient reference frame, and solves a minimum-time trajectory optimization problem. This is proven to be amenable to a closed-form solution, whose unknown parameters can be determined by solving numerically a nonlinear system of equations. Real time solution was found in all the simulations, thanks to the availability of a suitable guess for the unknown parameters. Furthermore, a new, nonlinear reduced-attitude control algorithm is introduced, which enjoys quasi-global stability properties, and is capable of driving the actual longitudinal axis toward the commanded thrust direction. Actuation is based on the use of thrust vectoring. Monte Carlo simulations prove that the guidance, control, and actuation architecture at hand is very effective for precise lunar orbit injection.

REFERENCES

1. A. J. Calise, N. Melamed, and S. Lee, "Design and evaluation of a three-dimensional optimal ascent guidance algorithm," J. Guid. Control Dynam. **21**(6), 867–875 (1998)
2. P. Lu, "Optimal Feedback Control Laws Using Nonlinear Programming," J. Opt. Theory & Appl. **71**(3), 599–611 (1991)
3. H. Seywald and E. M. Cliff, "Neighboring Optimal Control Based Feedback Law for the Advanced Launch System," J. Guid. Control Dynam. **17**(3), 1154–1162 (1994)
4. M. Pontani and F. Celani, F., "Neighboring optimal guidance and constrained attitude control applied to three-dimensional lunar ascent and orbit injection," Acta Astronaut. **156**, 78–91 (2019)
5. M. Pontani, G. Cecchetti, and P. Teofilatto, "Variable-Time-Domain Neighboring Optimal Guidance Applied to Space Trajectories," Acta Astronaut. **115**, 102–120 (2015)
6. P. C. Hughes, *Spacecraft Attitude Dynamics* (Dover Publications, Inc., Mineola, 2004), pp. 55–61